Food and Chemical Toxicology 135 (2020) 110900

Contents lists available at ScienceDirect

Food and Chemical Toxicology

journal homepage: www.elsevier.com/locate/foodchemtox

In vitro study of the protective effect of manganese against vanadium-mediated nuclear and mitochondrial DNA damage

Lorenzo Rivas-García[a,b], José L. Quiles[a], Alfonso Varela-López[a], Miguel Arredondo[c], Paulina Lopez[c], Antonio Rodríguez Diéguez[d], María Montes-Bayon[e], Pilar Aranda[a,b], Juan Llopis[a,b], Cristina Sánchez-González[a,b,*]

[a] Biomedical Research Centre, Institute of Nutrition and Food Technology, Department of Physiology, Faculty of Pharmacy, University of Granada, Avda. del Conocimiento s/n. 18071 Armilla, Granada, Spain
[b] Sport and Health Research Centre. University of Granada, C/. Menéndez Pelayo 32. 18016 Armilla, Granada, Spain
[c] Micronutrient Laboratory, Institute of Nutrition and Food Technology, University of Chile, Santiago de Chile, Chile
[d] Department of Inorganic Chemistry, University of Granada, Avda. Severo Ochoa s/n, Granada, 18071, Spain
[e] Department of Analytical Chemistry, Faculty of Chemistry, University of Oviedo, 33007, Oviedo, Spain

ARTICLE INFO

Keywords:
Vanadium
Manganese
DNA
Nucleus
Mitochondria
HepG2 cells

ABSTRACT

We aimed to study the effect of vanadium(V) exposure on cell viability, nuclear DNA (nDNA) and mitochondrial DNA (mtDNA) and to elucidate if these effects can be reverted by co-exposure to V and manganese (Mn). HepG2 cells were incubated with various concentrations of bis(maltolato)oxovanadium(IV) or MnCl2 for 32 h for viability study. The higher concentrations (59 μM V, 54 nM Mn and 59 μM V + 54 nM Mn) were used to study DNA damage and uptake of V and Mn. Comet assay was used for the study of nDNA damage; mtDNA damage was studied by determining deletions and number of copies of the ND1/ND4 mtDNA region. Cellular content of V and Mn was determined using ICPMS. Cellular exposure to 59 μM V decreased viability (14%) and damaged nDNA and mtDNA. This effect was partially prevented by the co-exposure to V + Mn. Exposure to V increased the cellular content of V and Mn (812.3% and 153.5%, respectively). Exposure to Mn decreased the content of V and Mn (62% and 56%, respectively). Exposure to V + Mn increased V (261%) and decreased Mn (56%) content. The positive effects on cell viability and DNA damage when incubated with V + Mn could be due to the Mn-mediated inhibition of V uptake.

1. Introduction

Vanadium(V) is a widely distributed element, which is essential for some living organisms. However, the role of V as micronutrient, its essentiality and its biological and pharmacological activities are still not completely understood (Domingo et al., 1991; Ścibior et al., 2012). The use of vanadium as an antidiabetic agent and as an anabolic agent due to its insulin-mimetic properties has been considered (Goldwaser et al., 2000; Thompson and Orvig, 2006). Moreover, environmental and occupational vanadium exposure has been associated with several health outcomes.

Many *in vivo* and *in vitro* studies have shown that different V compounds can inhibit various enzymes. Currently it is known that vanadate ions inhibit P-type ATPases (Nechay and Saunders, 1978; Aureliano, 2016). Recently, the inhibitory capacity of several polyoxometalates, such as polyoxotungstates (Gumerova et al., 2018) and polyoxovanadates, on ATPases has been shown. The phosphotetradecavanadate (PV_{14}) have shown a higher P-type ATPase inhibitory capacity than decavanadate (V_{10}) and monovanadate (V_1) (Fraqueza et al., 2019). Among other enzymes inhibited by these V compounds there are various phosphatases, ribonucleases, phosphodiesterases, phosphoglucomutase and glucose-6-phosphatase (McLauchlan et al., 2010; Treviño et al., 2019). Bis(maltolato)oxovanadium(IV) (BMOV) has been reported to be more effective than $VO(SO_4)$ as glucose-lowering agent and to be better tolerated in animal models. The use of V as antidiabetic agent is limited due to its pro-oxidant properties promoting certain toxicity (Domingo et al., 1995; Domingo and Gómez, 2016; Sanchez Gonzalez et al., 2012; Ścibior et al., 2006; Ścibior and Kurus, 2019). Vanadium (BMOV) exposure has been related to cytokine production (Sánchez-González et al., 2014), inflammatory changes in the upper and lower respiratory tracts intratracheally instilled with vanadyl sulfate $VO(SO_4)$ (Ghio et al., 2005, 2015) and lung tumors in workers

* Corresponding author. Department of Physiology, Campus Cartuja, University of Granada, E-18071, Granada, Spain.
E-mail address: crissg@ugr.es (C. Sánchez-González).

https://doi.org/10.1016/j.fct.2019.110900
Received 17 May 2019; Received in revised form 24 September 2019; Accepted 18 October 2019
Available online 22 October 2019

Table 1
Summary of the major events regarding V–Mn interactions.

Species	Vanadium compound	Concentration/dose	Administration period	Route	Side effects	Reference
Humans	V and Mn in road side dust	V (70 μg/g) Mn (511 μg/g)e Ratio V/Mn from 1:1 to 1:8	Occupational exposures	Inhaled	Neurobehavioral deficits	Barth et al. Cited by Bijelic et al. (2018)
Control rats and Diabetic rats	$NaVO_3$	1.2 mM/day	26 days	Drinking water	Liver and kidney Mn concentrations were not affected	Oster et al. (1993)
Diabetic rats	Sodium (4,4′-dimethyl-2,2′-bipyridine) oxooxidobisperoxovanadate(V) octahydrate (2,2′-bipyridine) oxooxido [tetraoxosulfato (2-)-O,O′] vanadium (IV) monohydrate	50 μmol/kg/day	5 weeks	Gavage	Increases the Mn content in the spleen	Krosniak et al. (2013)
Diabetic rats	Bis(maltolato)oxovanadium(IV)	0.75 mg/mL	5 weeks	Drinking water	Homeostasis of Mn was not affected	Sánchez-González et al. (2014)

exposed to high levels of V(V) in the form of V_2O_5 (Assem and Levy, 2012). However, other authors have suggested that several compounds of V(IV) and V(V) may mediate the inhibition of different forms of cancer (Das et al., 2012; Roy et al., 2018). A recent review study states that various polyoxometalates, such as $[V_{10}O_{28}]^{6-}$, show antitumor activity derived from its P-type ATPase inhibitory activity (Bijelic et al., 2019). In addition, the study of the antibacterial activity of various polyoxometalates, such as polyoxovanadotungstates and polyoxovanadates (especially decavanadate), have shown that some of them are more active than commonly used antibiotics (Bijelic et al., 2018).

Manganese (Mn) is a naturally occurring heavy metal essential for humans and animals. Manganese is a key component of different enzymes such as superoxide dismutase (SOD), which is present in mitochondrial cells. This is especially important because the respiratory chain is one of the processes producing free radicals in the cells, helping to avoid the effects of anion superoxide in the mitochondrial electron transport chain. Regarding V–Mn interactions, the information available is really scarce and it is summarized in Table 1.

The effect of exposure to vanadium, manganese or the combination of both elements on the integrity of nuclear and mitochondrial DNA remains unknown. It is known that several compounds of V(IV) and V (V) (Zhao et al., 2010; Hosseini et al., 2013; Cunha-de Padua et al., 2017) induce oxidative stress in mitochondria, which initiates cell apoptosis.

The uptake of both metals is mediated by divalent metal transporter 1 (DMT1) (Afeseh Ngwa et al., 2009; Gunshin et al., 1997; Mackenzie et al., 2007) and transferrin receptor (TfR). Both V and Mn are transported by transferrin (Iglesias-González et al., 2012; Treviño et al., 2019). Moreover, the expression of DMT1 could be modified by both; V (IV) in the form of $VOSO_4$ (Ghio et al., 2005) and V(V) in the form of V_2O_5 (Afeseh Ngwa et al., 2009) increase the expression of DMT1, whereas Mn decreases its expression (Bai et al., 2008).

According to the above and considering that cell nucleus and mitochondria are the main target cell organelles of V (Aureliano and Ohlin, 2014), and that Mn is essential for the antioxidant activity of mitochondrial SOD, the aim of the present study was to examine the changes in cell viability, the integrity of nuclear and mitochondrial DNA in HepG2 cells exposed to BMOV, and the effect of the co-exposure to BMOV and $MnCl_2$. The results obtained may help to clarify the biological role of vanadium, its toxicity and its pharmacological use.

2. Materials and methods

2.1. Preparation of the vanadium complex BMOV(IV), its characterization by electrospray ionization mass spectrometry, and biological ligands interaction studies by HPLC-ICP-MS

Instrumentation. The electrospray-ionization quadrupole time-of-flight (ESI-Q-TOF) mass spectrometry instrument used for addressing V (IV) complexation with the corresponding ligands is a QStar XL model (Applied Biosystems, Langen, Germany) equipped with an ion-spray source and using N_2 as nebulizing gas. The instrument was calibrated daily using renin standard. The samples were dissolved in 50% MeOH/H_2O and continuously injected at a flow of 5 μL/min.

The HPLC separations were performed using a dual piston solvent delivery pump (Shimadzu LC-10AD, Shimadzu Corporation, Kyoto, Japan) equipped with the sample injection valve Rheodyne Model 7125 (Cotati, CA, USA), fitted with a 100 μL injection loop, and an anion-exchange column, Mono-Q HR 5/5 (50 × 5 mm id, Pharmacia, Amersham Bioscience, Spain). Specific atomic detection of V in the column effluent was performed using an inductively coupled plasma mass spectrometer (ICP-MS) Model 4500 from Agilent Technologies (Agilent, Tokyo, Japan). Operating conditions are listed in Table 2. A scavenger column (25 × 0.5 mm id) was placed between the pump and the injection valve to eliminate possible traces of metal present as contamination in the mobile phases, thus the elemental contamination

Table 2
Instrumental operating conditions.

HPLC parameters	
Column	Mono Q 5/5 HR (Pharmacia, Amersham)
Mobile phases	A. 50 mM Tris-Acetic Acid (pH 7)
	B. A + 250 mM Ammonium Acet. buffer (pH 7)
Gradient	0%–100% B in 30 min
	30–35 min 100% B
	36 min 0%B
Injection volume	100 μL
Flow rate	1 mL/min
Detection	UV (295 nm)
ESI-MS parameters	
Instrument	QStar XL (Applied Biosystems)
Scan type	Positive TOF MS or Positive Product Ion
Ionspray voltage	5.5 kV
Nebulizing gas	N_2
Injection rate	5 μL/min
External calibration	Renin standard

coming from the chromatographic system is reduced. The scavenger column was packed with Kelex-100 (Schering, Germany) impregnated silica C18 material (20 μm particle size) (Bondapack, Waters Corporation, Massachusetts, USA).

Preparation of the complex. The vanadyl complex BMOV was synthesized as previously described [26]. Briefly, the vanadyl complexes were synthesized by adding the stoichiometric amount of vanadyl sulfate and the corresponding ligand in water, adjusting the pH to 9 and leaving to stand for 1 h. Characterization was conducted by ESI-Q-TOF.

2.2. Stability of BMOV determined by NMR

The stability of BMOV in the culture medium was determined by nuclear magnetic resonance (NMR). A Bruker Avance NEO 500 MHz instrument (Ettlingen, Germany) was used. Crystals of the ligand 3-Hydroxy-2-methyl-4-pyrone, 3-Hydroxy-2-methyl-4H-pyran-4-one (maltol) and BMOV were dissolved in deuterated water and cell culture medium (RPMI) with 10% deuterated water.

2.3. Exposure to vanadium and manganese

Cells were incubated with BMOV at the following concentrations of V: 7, 15, 29 and 59 μM. For manganese studies, cells were incubated with $MnCl_2$ at the following concentrations of Mn: 18, 36 and 54 nM. The selection of doses in this study were calculated based on the serum concentration found in *in vivo* studies (Sanchez Gonzalez et al., 2012, 2014). The Mn concentrations correspond to the physiological levels in plasma, twofold and threefold. Viability was tested at all the proposed concentrations of metals. However, only the highest concentration of each metal and the combination of both metals were used for the mtDNA and comet assays. Cells were incubated with the metals for 32 h for all these studies.

2.4. Cell culture conditions

The HepG2 cell line was obtained from the Cell Culture Resource Centre at the University of Granada (Spain). Cells were precultured in 25 cm^2 culture flasks at 37 °C in RPMI 1640 medium (Sigma) with 10% (v/v) fetal bovine serum and 2 mM glutamine in a humidified atmosphere of 5% CO_2. The culture medium for HepG2 was replaced once per day. After the cell density reached 20^3 cell/mL approximately, HepG2 cells were detached by trypsinization using a 0.25% trypsin-EDTA solution, and collected by centrifugation at 1500 rpm for 5 min. Cell density was determined using a Neubauer chamber.

2.5. Cell viability assay

For determining cell viability, HepG2 cells were allowed to grow until 60% confluence was reached. Subsequently, a (3-(4,5-dimethylthiazol-2-yl)-2,5-diphenyltetrazolium bromide) (MTT) assay was performed according to the method developed by Mossman in 1983 and modified by Denioz and Lamb (Denizot and Lang, 1986). Briefly, after adding 100 μL of MTT (0.5 mg/mL) to each well, the mixtures were incubated for 4 h at 37 °C. The supernatant was aspirated, and the MTT-formazan crystals were formed by metabolically viable cells and were dissolved in 100 μL of DMSO under 15 min incubation. Finally, the absorbance was measured using a microplate reader at a wavelength of 570 nm. The relative cell viability was calculated compared to control wells containing only medium. All experiments were performed in triplicate.

2.6. Comet assay

HepG2 cells were allowed to grow until 60% confluence was reached. Subsequently, cell cultures were exposed to 59 μM BMOV, 54 nM $MnCl_2$, and the combination of 59 μM BMOV and 54 nM $MnCl_2$ for 32 h. Positive control cells were treated with 100 mM H_2O_2 for 1 h. Upon treatment, cells were treated with trypsin–EDTA solution (Sigma, St Louis, MO, USA) and centrifuged for pellet collection. Cells were resuspended in 1 mL PBS.

Microscope glass slides were pre-coated with 1% normal melting point (NMP) agarose on one side. A total of 30 μL of cell suspension were mixed with 65 μL of low melting point (LMP) agarose solution (final LMP agarose concentration 0.5%). Drops of each agarose-cell suspension were added on each pre-coated slide and placed for 1 h at 4 °C in the lysis solution (containing NaCl 2.225 M, Na_2EDTA 88.9 mM, Tris 8.8 mM, NaOH 0.22 M, 10% DMSO and 1% Triton X-100). Electrophoresis (1 V/cm) was performed for 20 min at 4 °C using an electrophoresis solution (Na_2EDTA 1 mM and NaOH 300 mM, pH > 13).

The solution of the slide was neutralized in triplicate (5 min every time) with Tris 0.4 M. Ethanol was used for fixation. Finally, samples were stained with 2-(4-amidinophenyl)-1H -indole-6-carboxamidine (DAPI) (1 μg/mL) and analyzed using a fluorescence microscope (Eclipse Ni; Nikon Instruments Europe B.V., Badhoevedorp, The Netherlands). Over 150 nucleoids per sample (50 nucleoids per slide) stained with DAPI were scored by computerized image analysis (CaspLab, University of Wrocalw, Poland). Cells containing damaged DNA have the appearance of a comet with a bright head and tail. In contrast, undamaged DNA appears as an intact nucleus with no tail. DNA damage was determined by comparing tail moments among groups.

2.7. Assessment of the proportion of deleted mtDNA and mtDNA copy number

The proportion of deleted mtDNA was determined using a quantitative reverse-transcription polymerase chain reaction (QRT-PCR) to amplify two mitochondrial genes, MT-ND4 and MT-ND1. Relative levels of mtDNA copy number were also determined using QRT-PCR by amplifying the single-copy nuclear gene acidic ribosomal phosphoprotein P0 (36B4) and using the previously obtained amplification data of mitochondrial MT-ND1 gene. DNA amplification was performed in a MicroAmp Optical 384-well Reaction Plate (Applied Biosystems, Foster City, CA, USA) using the Applied Biosystem's 7900HT Fast Real-Time PCR system. Primers used for the assays were as follows: MT-ND1 forward 5′-CCCTAAAACCCGCCACATCT′-3, MT-ND1 reverse GAGCGA TGGTGAGAGCTAAGGT-3′, MT-ND4 forward 5′-CCATTCTCCTCCTATC CCTCAAC-3′, MT-ND4 reverse 5′-CACAATCTGATGTTTTGGTTAAACT ATATTT-3′, 36B4 forward 5′-CTGCAGATTGGCTACCCGAC-3′ and 36B4 reverse 5′-CACAGACAAAGCCAGGACCC-3′. Final primer

concentrations were 200 nM except for the last two that concentrations were 300 and 500 nM, respectively. Reactions were performed in a total volume of 10 µL. Reaction mixture in each well included genomic DNA (5 ng), 2x QuantiNova SYBR Green PCR Master Mix (Applied Biosystems, Foster City, CA, USA) (5 µL), ROX dye (Applied Biosystems, Foster City, CA, USA) (1 µL), Mili-Q sterilized H2O and the corresponding oligonucleotide primers. Reaction conditions were set at 95 °C for 2 min followed by 40 cycles of data collection consisting of a denaturation step at 95 °C for 8 s and an annealing/extension at 58 °C for 15 s. An additional phase to obtain a melting curve was performed at the end of each reaction to verify specific amplification. Standard curves were included for data analysis. Mean quantification cycle (Cq) for each sample was calculated using Sequence Detector Systems version 2.4 software. The proportion of deleted mtDNA was calculated for each well as the ratio between MT-ND4 and MT-ND1 amplification data considering reaction efficiency values. The resulting values were divided by the average obtained from control samples (untreated cells) analysis. This allowed to obtain a relative MT-ND4:MT-ND1 ratio. In turn, the MT-ND1:36B4 ratio was calculated and multiplied per two to obtain mtDNA copy number for each sample. DNA used in the aforementioned assays was isolated using a NucleoSpin Tissue kit (Macherey-Nagel GmbH & Co. KG, Dóren, Germany) according to the manufacturer's instructions.

2.8. Determination of total metal concentrations

First, HepG2 cells were washed with physiological saline solution, and then diluted with a basic solution containing ammonium hydroxide, butanol, EDTA and Triton X-100. Determination of V, Mn and Fe total content in cells samples was performed using an ICP-MS instrument (Agilent 7500, Agilent Technologies, Tokyo, Japan) fitted with a Meinhard type nebulizer (Glass Expansion, Romainmotier, Switzerland) and equipped with a He collision cell. A Milli-Q system (Millipore, Bedford, MA, USA) was used to obtain deionized water (18 MΩ). All reagents (Ammonium Hydroxide Solution, Butanol, EDTA, Triton X-100) used were of the highest purity available. A standard solution of 100 µg/L of Li, Mg, Sc, Co, Y, In, Ce, Ba, Pb, Bi, and U in 1% (v/v) HNO3 was prepared from a 1000 mg/L multi-element stock standard solution (Merck) and used for daily optimization of the ICP-MS parameters. Single-element standard solutions for ICP-MS containing 1000 µg/mL of V, Mn and Fe were also purchased from Merck. Calibration curves were prepared using Ga as an internal standard and by the dilution of stock solutions of 1000 mg/L in 1% HNO3. The accuracy of this method was evaluated by comparison with the certified reference material SeronormTM Trace Elements Serum (Billingstad, Norway) and by recovery studies of spiked samples with multi-element standards. The calculated recoveries for each element were between 95% and 105% in all cases. The percentage of the coefficient of variation (CV) obtained was 5.6% for V, 1.3% for Fe and 2.9% for Mn. For each element, we used the mean of five separate determinations of this reference material.

2.9. Statistical analysis

Descriptive statistical parameters (means and standard deviations of 8 samples for each experiment) were obtained for each of the variables studied. The means of independent variables were statistically compared among the groups. All analyses were performed using SPSS 20.0 (SPSS, Chicago, IL, USA). Differences were considered statistically significant at a probability level < 5%.

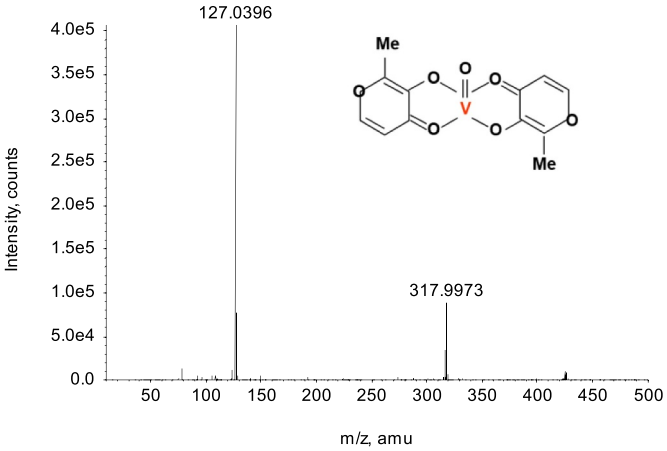

Fig. 1. Characterization of BMOV by electrospray ionization mass spectrometry.

3. Results

3.1. Characterization of BMOV by electrospray ionization mass spectrometry

The presence of V(IV) complexes was assessed by ESI-Q-TOF. For this purpose, the samples were dissolved in 50% MeOH/water and directly introduced into the instrument. Fig. 1 shows the spectra corresponding to BMVO. As it can be observed, the main product is the expected complex with molecular ion at m/z 318 and the excess of maltol at m/z 127 showing also mass defect characteristic of V. The structure of these species was further confirmed by MS/MS (data not shown).

Incubation of BMOV with transferrin. The standard of transferrin was used as purchased without further purification. Solutions (0.5 µL) containing 3 mg/mL of transferrin were incubated with 0.5 µL of the V (IV) (10 µg/mL) complex at 37 °C for 24 h. After incubation, samples were measured directly by HPLC-ICP-MS. The mixtures were degassed to avoid possible V oxidation by passing a gentle flow of N_2 over the surface of the solution prior sample manipulation. All incubations were performed in the presence of a 25 mM $NaHCO_3$ (25 µL) solution). Fig. 2 shows a single peak corresponding to the vanadyl-saturated transferrin.

3.2. BMOV stability in cell culture medium

The results of the NMR assay show that BMOV was stable over several days without any sign of decomposition. The ^{1}H-NMR spectrum (23 °C) of the ligand maltol dissolved in deuterated water shows a number of resonances (Fig. 3a). Likewise, maltol dissolved in RPMI

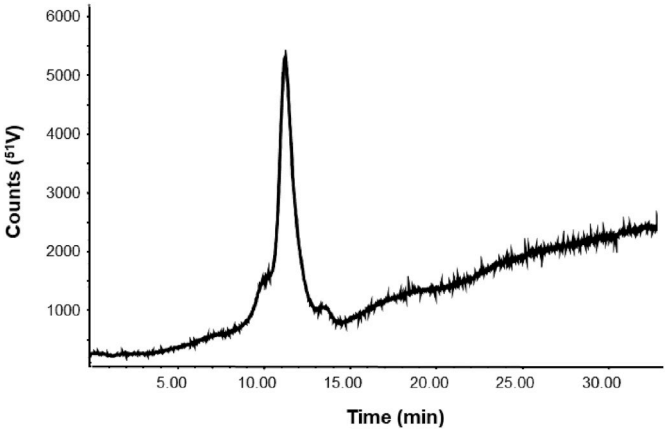

Fig. 2. HPLC-ICP-MS profile after incubation of BMOV with transferrin.

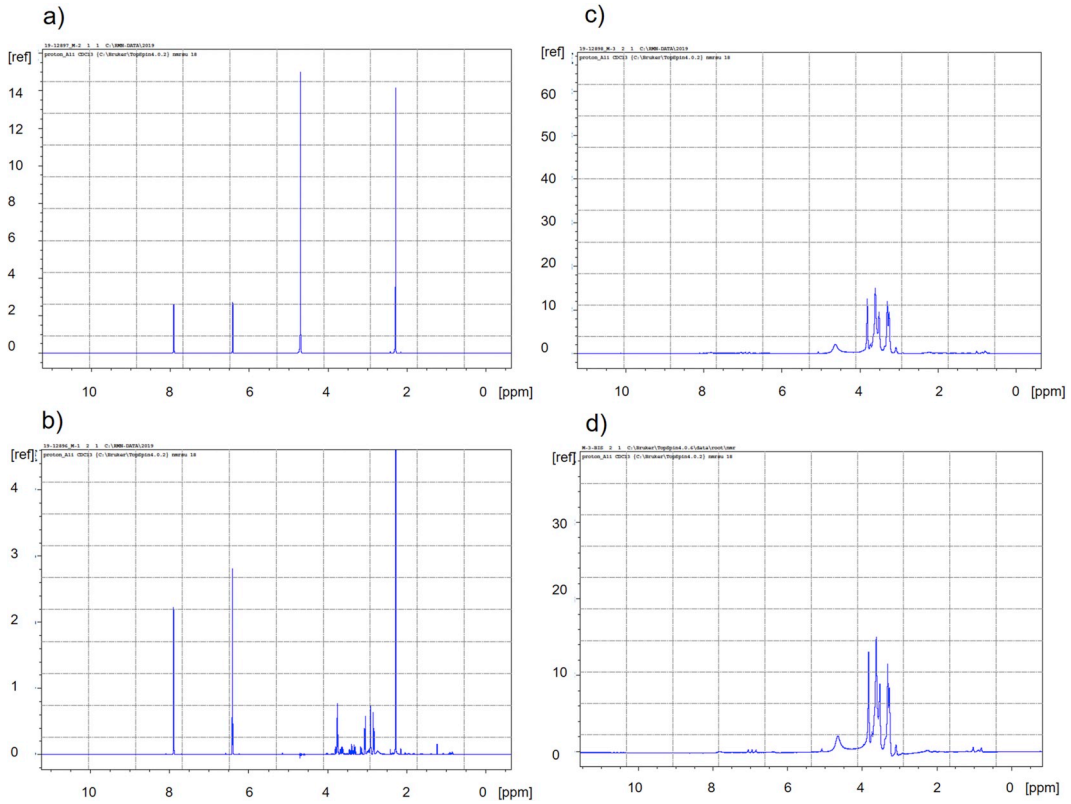

Fig. 3. NMR spectra to corroborate the stability of BMOV in RPMI medium.

showed the same ^{1}H-NMR spectrum in addition to a number of resonances consistent with the composition of the cell culture medium (Fig. 3b). Interestingly, when BMOV was dissolved in the culture medium (Fig. 3c), the signals corresponding to the ligand maltol were not found. BMOV is a paramagnetic complex, the non-appearance of these signals is an unequivocal proof that the compound BMOV remained in solution. Finally, after 48 h, the spectrum of the compound BMOV in the culture medium (Fig. 3d) was recorded again, finding that this compound was stable over several days without any sign of decomposition.

3.3. Cell viability

Fig. 4 shows the results of cell viability according to the MMT assay in HepG2 cells incubated with different concentrations of V or Mn. When HepG2 cells were incubated with V at doses above 7 μM, a significant decrease in cell viability was observed in a dose dependent manner (Fig. 4). No significant differences were found in cell viability when cells were exposed to 18 nM Mn compared to unexposed cells. However, cell viability increased significantly when cells were exposed to 36 and 54 nM Mn (Fig. 4). The co-exposure of HepG2 cells to BMOV and $MnCl_2$ (Fig. 5) caused a significant increase in cell viability compared to the viability found in control cells and cells exposed to 59 μM BMOV.

3.4. DNA damage

Results of the tail moment of the comet assay are shown in Table 3

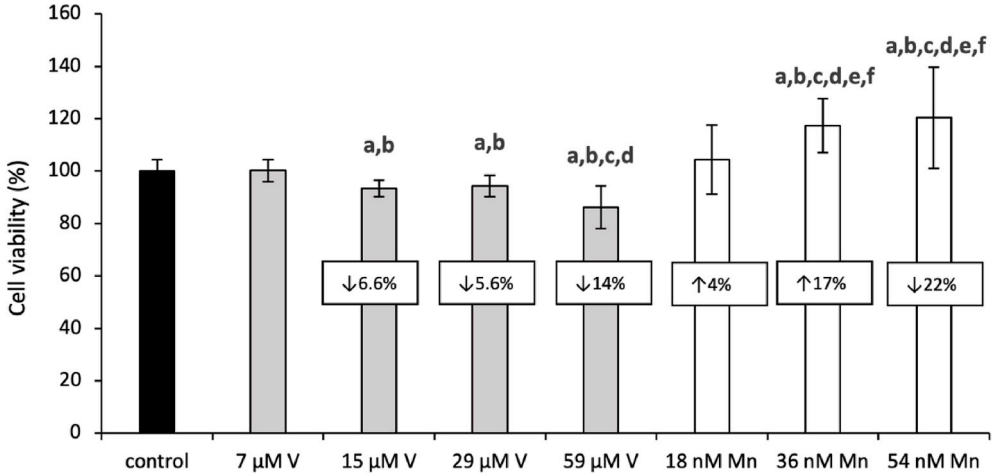

Fig. 4. Cell viability of HepG2 Cells in presence of BMOV or $MnCl_2$. Results expressed as mean ± SD. (a) *vs.* control group; (b) *vs.*7 μM V; (c) *vs.*15 μM V, (d) *vs.* 29 μM V; (e) *vs.* 59 μM V; (f) *vs.* 18 nM Mn. $p < 0.05$. Percentage rate of decrease (↓) or increase (↑).

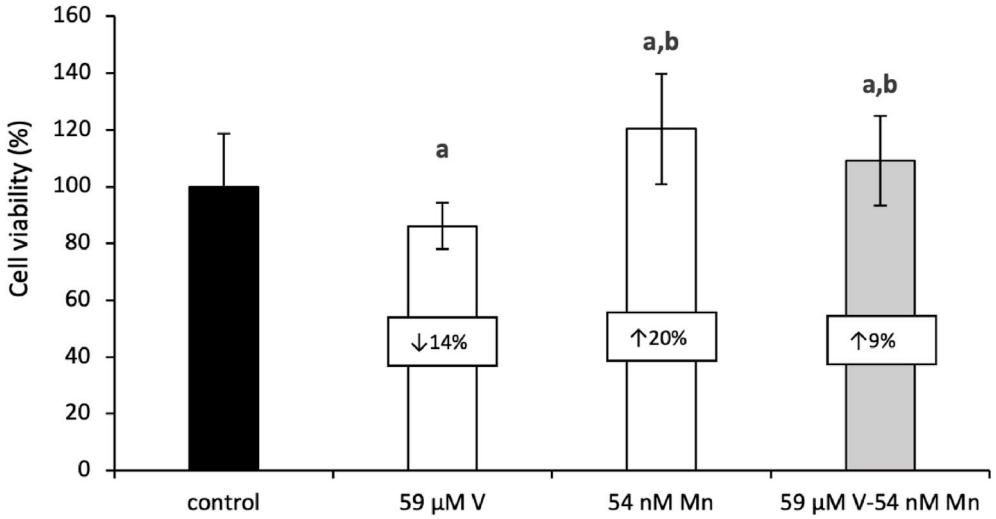

Fig. 5. Cell viability of HepG2 Cells in presence of BMOV or MnCl2. Results expressed as mean ± SD. (a) *vs.* control group; (b) *vs.* 59 µM V. $p < 0.05$. Percentage rate of decrease (↓) or increase (↑).

Table 3
Tail moment values. Comets from HepG2 cells. Results expressed as mean ± SD. (a) *vs.* control; (b) *vs.* positive control (H_2O_2); (c) *vs.* 59 µM V; (d) *vs.* 54 nM Mn. $p < 0.05$

	Tail moment value
Control	2.59E-02
Positive control cells (H_2O_2)	91.49^{a}
Cells exposed to 59 µM V	39.44^{ab}
Cells exposed to 54 nM Mn	0.0302^{bc}
Cells exposed to 59 µM V + 54 nM Mn	26.78^{abcd}

and Fig. 6. In cells exposed only to BMOV, tail moment value increased significantly compared to all groups ($P < 0.05$).

The tail moment of cells incubated with $MnCl_2$ was similar to that found in control cells. Finally, cells incubated with the combination of BMOV and $MnCl_2$ showed a tail moment value significantly lower than that found in cells incubated only with V.

3.5. Proportion of deleted mtDNA and mtDNA copy number

Regarding the proportion of deleted mtDNA, cells exposed to V showed higher relative MT-ND1:MT-ND4 ratio than those cells belonging to the control group and those exposed to Mn alone or to the combination of V and Mn (Fig. 7).

In turn, differences in mtDNA copy number values were found between control and V-treated cells. However, no statistically significant differences in this parameter were found between cells treated with Mn alone or V and Mn combination and those from control or V exposed groups (Fig. 8) (see Fig. 9).

3.6. Fe, Mn and V uptake

The cellular uptake of V and Mn was determined. In addition, the cellular uptake of Fe was measured because this metal uses the same membrane transporter than Mn and could be involved in the process. Table 4 shows the results of the cellular uptake assays performed, showing the presence of significantly higher levels of V, Mn and Fe in cells incubated with 59 µM BMOV. Nevertheless, the exposure of cells to 54 nM $MnCl_2$ decreased significantly the levels of the three studied metals compared to control cells or cells incubated with V. When cells were incubated with a combination of 59 µM BMOV and 54 nM $MnCl_2$, the V cellular levels found were higher compared to those found in control cells and cells incubated only with Mn, but lower than those

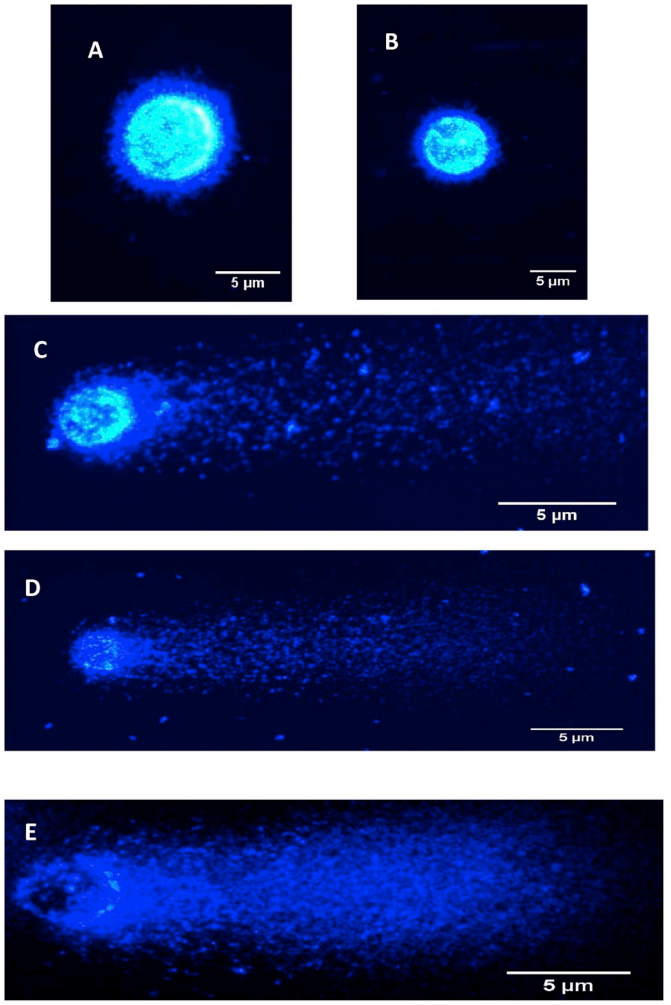

Fig. 6. Comets from HepG2 cells. (A) control unexposed cells; (B) cells exposed to 54 nM Mn; (C) cells exposed to 59 µM V + 54 nM Mn; (D) cells exposed to 59 µM V; (E) Positive control cells exposed to H_2O_2.

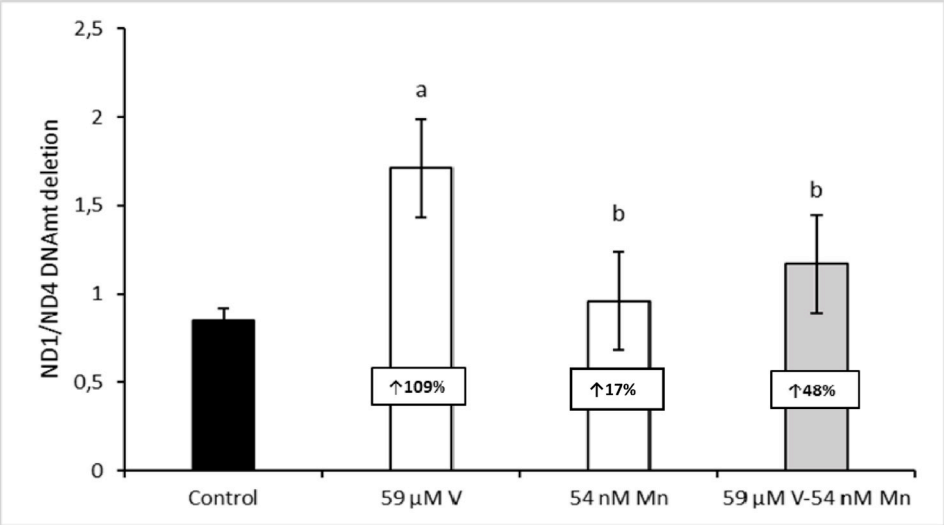

Fig. 7. ND1/ND4 mtDNA deletion. Results expressed as mean ± SD. (a) *vs.* control; (b) *vs.* 59 µM V. $p < 0.05$. Percentage rate of decrease (↓) or increase (↑).

found in cells incubated only with V. No differences in the levels of Mn and Fe were found between both groups treated with Mn.

4. Discussion

4.1. Stability of BMOV

The results show that the vanadium complex synthesized and used in the present study is stable in our experimental conditions. The *ex vivo* interaction between BMOV and transferrin shows the ability of BMOV to interact with biological ligands becoming part of the internal environment.

4.2. Cell viability

A decrease in the viability of HepG2 cells exposed to 15, 29 and 59 µM BMOV (Fig. 4) could be associated with the prooxidant and proinflammatory activity of V suggested by other authors (Sanchez Gonzalez et al., 2014; Ścibior and Kurus, 2019). The exposure of cells to 36 and 54 nM Mn significantly increased cell viability. This increase can be explained by the protective properties associated with this metal on which the activity of the mitochondrial SOD enzyme is dependent (Fig. 4). A higher cell viability was found in cells incubated with a combination of both metals (V and Mn) compared to unexposed control cells, reaching levels similar to those found in cells incubated with only Mn. This fact suggested that the dose of Mn studied is able to compensate the oxidant effects of V (Fig. 5).

4.3. Nuclear DNA damage

Previously published studies conducted *in vivo* have shown that BMOV (IV) promoted the oxidative stress causing lipid peroxidation and protein carbonylation (Sanchez Gonzalez et al., 2012). In order to deepen this concept, oxidative nuclear DNA damage was studied by the determination of the parameter "tail moment" using the comet assay. The experimental conditions were the same than those used for the viability assays (HepG2 cells incubated with 59 µM BMOV, 54 nM $MnCl_2$, and the combination of both). Tail moment increased significantly (more than 1500 times) in hepatocytes incubated with 59 µM BMOV showing DNA damage compared with unexposed cells (Table 3,

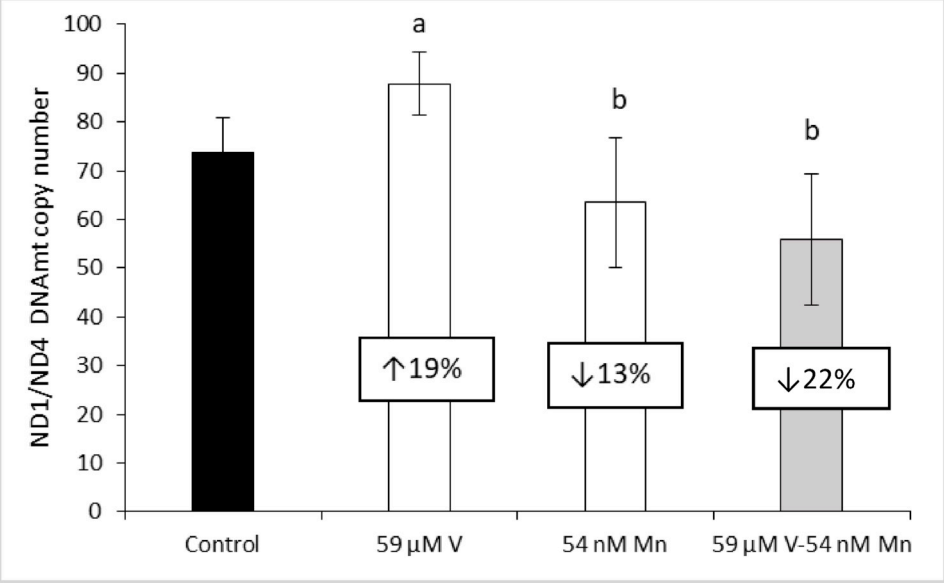

Fig. 8. ND1/ND4 mtDNA copy number. Results expressed as mean ± SD. (a) *vs* control. $p < 0.05$. Percentage rate of a decrease (↓) or increase (↑).

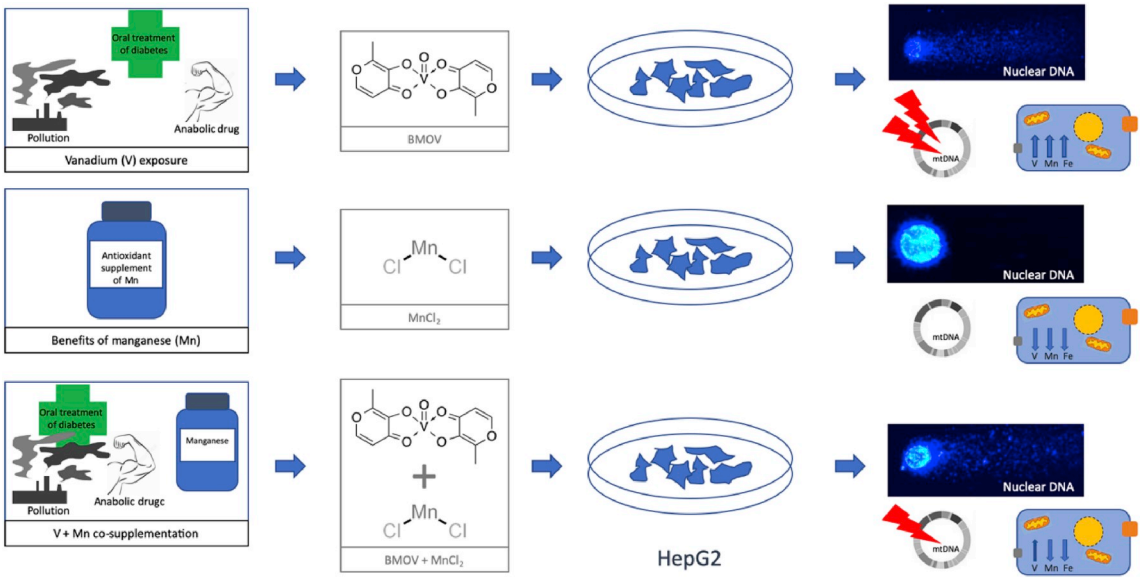

Fig. 9. Chart of the major effects and applications of vanadium and manganese.

Table 4
HepG2 cellular content of V, Mn and Fe after 32 h incubation with V, Mn and V + Mn. Results expressed as mean ± SD. (a) *vs.* control; (b) *vs.* 59 μM V; (c) *vs.* 54 nM Mn

Exposure levels to V or/ and Mn	Cellular metal content		
	V ng/10^6 cells	Mn ng/10^6 cells	Fe ng/10^6 cells
Control	5.54 ± 0.06	43 ± 12	6393 ± 144
59 μM V	45 ± 0.38[a]	66 ± 1.3[a]	9616 ± 86[a]
54 nM Mn	2.12 ± 0.028[a,b]	19 ± 0.11[a,b]	2514 ± 31[a,b]
59 μM V + 54 nM Mn	14.47 ± 0.28[a,b,c]	20 ± 0.48[a,b]	2610 ± 68[a,b]

Fig. 6). This result is consistent with the decrease in cell viability found in cells exposed to this dose of BMOV. The findings are consistent with those previously described by other authors who found that V (IV) tetraoxide (V_2O_4) damaged chromosomes or found an increase in comet tail length in splenocytes of mice caused by vanadium administered as sodium ortho-vanadate (V) (Leopardi et al., 2005). Moreover, it has been shown that V induced sperm nuclear DNA fragmentation (Vijaya Bharathi et al., 2015) and a tight interaction of VO-complexes with the DNA (Adam and Elsawy, 2018). Nuclear DNA was not altered when cells were incubated with 54 nM $MnCl_2$. The absence of nuclear DNA damage would keep cell viability intact, as shown in the results obtained in the present study (Fig. 4). Tail moment value decreased (by 32%) when cells were incubated with BMOV and $MnCl_2$ simultaneously (Table 3, Fig. 6) compared with cells treated with only BMOV. Nonetheless, this effect was not predicted by the MTT assay, whose results showed that in cells incubated with both metals at the same time, cell viability was higher to that found in control unexposed cells.

4.4. Mitochondrial DNA damage

Mitochondria are the main cell source of reactive oxygen species (ROS) and this organelle is very susceptible to oxidative stress. Vanadium can accumulate in mitochondria, which depends on the concentration of V, exposure time and tissue type (Aureliano and Ohlin, 2014; Soares et al., 2007). The role of vanadium in mitochondria has not yet be clarified. It has been described how mitochondria isolated from rat liver exposed to V (IV) or V (V) exhibited multiple actions on mitochondria. These effects included the induction of ROS formation, ATP depletion, mitochondrial permeability transition pore (PTP) opening and apoptosis induction by cytochrome *c* release (Hosseini et al., 2013; Zhao et al., 2010). Other studies have shown how different V formulations (as decavanadate) affected the redox state of the mitochondrial complex III without changes in complex IV nor inducing the opening of the mitochondrial permeability transition pore (Aureliano and Ohlin, 2014). However, there is currently no information on whether BMOV affects mtDNA or the capacity of Mn to prevent potential damages. In the present study, the toxic effect of BMOV on mitochondria was evaluated using ND1/ND4 deletion and variations in mtDNA copy number. Integrity of mtDNA has been related to mitochondrial function and involved in conditions such as diabetes, cancer or neurodegenerative disorders (Sharma and Sampath, 2019; Yamada et al., 2006; Yu, 2011). Aging has been also associated with increases in mtDNA deletions (Picard et al., 2016). Meanwhile, dietary treatments such as calorie restriction (Cassano et al., 2004) or feeding on various unsaturated fats (Ochoa et al., 2011; Quiles et al., 2010, 2006) attenuated mtDNA deletions in aging. The MT-ND4 gen is within the so-called common deletion and the ratio with the most stable MT-ND1, rarely deleted, correlates with the level of deleted mtDNA (He et al., 2002). In the present study, a higher relative MT-ND1:MT-ND4 ratio (Fig. 7) was found in cells exposed to BMOV (59 μM) compared to the control cells. Vanadium (IV) and (V) induce mitochondrial ROS formation (Hosseini et al., 2013; Zhao et al., 2010), which could lead to more oxidative alterations of DNA, including deletions, which are supported by differences in MT-ND1:MT-ND4 ratio found in this study. This deleterious effect of BMOV on mtDNA is consistent with the higher nuclear DNA damage as demonstrated by the results of the comet assay. Therefore, the damage to HepG2 cells affected the mitochondrial and nuclear DNA structure. Both types of damage were prevented after the concomitant exposure to V and Mn. Furthermore, mtDNA copy number reached similar results to those found for mtDNA deletion (Fig. 8). Therefore, the exposure to BMOV increased mtDNA copy number, and additional exposure to $MnCl_2$ (i.e. V 59 μM + Mn 54 nM) reduced it. The replication of mtDNA may not be associated with mitochondrial proliferation in all situations (Shadel, 1997). However, mtDNA replication is regulated by genes involved in mitochondrial biogenesis, such as the mitochondrial transcription factor A (TFAM), which is directly proportional to the mtDNA amount (Ekstrand et al., 2004; Pohjoismäki et al., 2006). In the present study, toxic effects of BMOV on mitochondria led to an increased mtDNA copy number, which might be the cellular response to an increased process of selective mitophagy (Kim et al., 2007). Therefore, biogenesis would be stimulated to compensate the decline in mitochondrial function (Lee and Wei, 2005). The

lower activation of biogenesis suggests that this effect is occurring in the present study.

4.5. Fe, Mn and V uptake

The effect of metals on cell viability and nDNA and mtDNA could be explained by the cellular uptake and homeostasis of metals. The cellular concentration of V, Mn and Fe were determined to quantify this uptake. The Fe levels have been analyzed because V, Mn and Fe are transported in blood by transferrin (Tf) (Horning et al., 2015) and the three of them use the same mechanisms for their cellular uptake (mainly DMT1 and TfR1); in addition, ferroportin (FPN1) is involved in the efflux of both Fe and Mn (Horning et al., 2015).

It is known that the divalent metal transporter 1 (DMT1) plays an important role in cellular uptake of Fe^{2+}, Mn^{2+} (Gunshin et al., 1997) and V (as V^3 o VO^{2+}) (Afeseh Ngwa et al., 2009; Mackenzie et al., 2007). However, the effect of V on the expression of the transporter is not fully understood. No significant changes in the DMT1 levels have been found in the liver and in the cerebral hemispheres of rats exposed to V(V) in the form of $NaVO_3$, supplied in their drinking water; whereas the kidney levels of DMT1 decreased in these rats compared to control rats (Scibior et al., 2014). In contrast, other authors (Ghio et al., 2015) reported an increased expression of the DMT1 in human bronchial epithelial cells after an exposure to V(IV) in the form of $V(SO_4)_2$. Consequently, the increase in V, Mn and Fe cellular levels when cells are incubated with BMOV (Table 4) could be caused by several processes. The increased expression of DMT1 (Ghio et al., 2015), which facilities the uptake of the three metals in the divalent form, particularly Mn(II) and Fe(II). The formation of the ferrous ion (Fe(II)) from the ferric ion (Fe(III)) present in the cell growth media could be due to the complex redox chemistry of vanadium allowing the oxidation of V (IV) to V(V) with the subsequent reduction of Fe(III) to Fe(II). This would explain a higher Fe(II) uptake through DMT1. Simultaneously, the oxidized V(V) could be taken up in association with Tf through TfR1 (Treviño et al., 2019). Our research group have previously showed that BMOV increases gene expression of hepcidin in liver (Sanchez Gonzalez et al., 2014). Hepcidin produces the degradation of FPN1 (De Domenico et al., 2007; Nemeth et al., 2004), which could decrease the efflux of Mn and Fe, leading to the accumulation of these metals into the hepatic cells. In cells incubated with $MnCl_2$, a significant decrease in the concentration of V, Mn and Fe compared to control cells has been found (Table 4). In this case, the hypothesis states that Mn(II) and Fe(III) compete for the binding sites of Tf. This fact induces a decrease in the uptake of Fe(III) uptake because it can only be taken up by means of Fe-Tf complex formation. Moreover, an inhibition of Fe uptake has been found (Arredondo et al., 2013) in DMT1-transfected HEK-293 cells after an exposure to Mn. Other authors have suggested that Mn promoted a decrease in DMT1 mRNA expression (Bai et al., 2008), and an increase in FPN1 mRNA expression in Caco-2 cells treated with Mn (Li et al., 2013). Consequently, a decrease in DMT1 expression could be associated with a lower metal uptake and an increase in FPN1 expression will result in an increase of the efflux of Mn and Fe. Thus, all mechanistic pathways can be occurring at the same time when the two metals (V + Mn) are provided simultaneously. Therefore, the positive effects on DNA and cell viability shown in this study when cells were incubated with $MnCl_2$ and BMOV compared with cells incubated only with BMOV could be due to the Mn-mediated inhibition of V uptake.

5. Conclusion

In conclusion, at the experimental conditions of this study, the exposure of HepG2 cells to 59 μM V, administered as BMOV (IV), decreased cell viability and caused significant nDNA and mtDNA damage. These negative effects were partially corrected by the co-exposure of cells to 59 μM V and 54 nM Mn, the latter administered as $MnCl_2$, in the culture medium. These co-exposure effects could be due to the fact that Mn significantly decreases the cellular uptake of V. The possible positive association of both trace elements V and Mn could facilitate the therapeutic use of V and reduce the toxicity of the V from the environmental and occupational vanadium exposure. Nevertheless, further studies are needed to better determine the effects arising from these interactions to establish the role of V as a micronutrient and to reduce its toxic effects. Future assays will be conducted to establish the functionality of the mitochondria in mitochondrial respiration as a consequence of the mtDNA damage induced by vanadium and restored after the exposure to manganese.

Declaration of competing interest

The authors declare that they have no known competing financial interests or personal relationships that could have appeared to influence the work reported in this paper.

Acknowledgements

We are grateful for the support received from the Consejería de Innovación, Ciencia y Empresa, Andalusian Regional Government (Project P06-CTS-01435). Some of the presented results are included in the PhD thesis dissertation of Lorenzo Rivas García from the University of Granada, Nutrition and Food Sciences Doctoral Program. We acknowledge Nutraceutical Translations for English language editing of this manuscript.

References

Adam, M.S.S., Elsawy, H., 2018. Biological potential of oxo-vanadium salicylidene amino-acid complexes as cytotoxic, antimicrobial, antioxidant and DNA interaction. J. Photochem. Photobiol. B Biol. 184, 34–43. https://doi.org/10.1016/j.jphotobiol.2018.05.002.

Afeseh Ngwa, H., Kanthasamy, A., Anantharam, V., Song, C., Witte, T., Houk, R., Kanthasamy, A.G., 2009. Vanadium induces dopaminergic neurotoxicity via protein kinase Cdelta dependent oxidative signaling mechanisms: relevance to etiopathogenesis of Parkinson's disease. Toxicol. Appl. Pharmacol. 240, 273–285. https://doi.org/10.1016/j.taap.2009.07.025.

Arredondo, M., Muñoz, P., Mura, C.V., Núñez, M.T., 2013. DMT1, a physiologically relevant apical Cu 1+ transporter of intestinal cells. Am. J. Physiol. Cell Physiol. 284, C1525–C1530. https://doi.org/10.1152/ajpcell.00480.2002.

Assem, F.L., Levy, L.S., 2012. Inhalation toxicity of vanadium. In: Michibata, H. (Ed.), Vanadium: Biochemical and Molecular Biological Approaches. Springer Netherlands, Dordrecht, pp. 209–224.

Aureliano, M., Ohlin, C.A., 2014. Decavanadate in vitro and in vivo effects: facts and opinions. J. Inorg. Biochem. https://doi.org/10.1016/j.jinorgbio.2014.05.002.

Aureliano, M., 2016. Decavanadate toxicology and pharmacological activities: V10 or v1, both or none? Oxid. Med. Cell. Longev. https://doi.org/10.1155/2016/6103457.

Bai, S.P., Lu, L., Luo, X.G., Liu, B., 2008. Kinetics of manganese absorption in ligated small intestinal segments of broilers. Poult. Sci. 87, 2596–2604. https://doi.org/10.3382/ps.2008-00117.

Bijelic, A., Aureliano, M., Rompel, A., 2019. Polyoxometalates as potential next-generation metallodrugs in the combat against cancer. Angew. Chem. Int. Ed. https://doi.org/10.1002/anie.201803868.

Bijelic, A., Aureliano, M., Rompel, A., 2018. The antibacterial activity of polyoxometalates: structures, antibiotic effects and future perspectives. Chem. Commun. https://doi.org/10.1039/c7cc07549a.

Cassano, P., Lezza, A.M.S., Leeuwenburgh, C., Cantatore, P., Gadaleta, M.N., 2004. Measurement of the 4,834-bp mitochondrial DNA deletion level in aging rat liver and brain subjected or not to caloric restriction diet. In: Annals of the New York Academy of Sciences, pp. 269–273.

Cunha - de Padua, M.M., Suter Correia Cadena, S.M., de Oliveira Petkowicz, C.L., Martinez, G.R., Merlin Rocha, M.E., Mercê, A.L.R., Noleto, G.R., 2017. Toxicity of native and oxovanadium(IV/V) galactomannan complexes on HepG2 cells is related to impairment of mitochondrial functions. Carbohydr. Polym. 173, 665–675. https://doi.org/10.1016/j.carbpol.2017.06.027.

Das, S., Chatterjee, M., Janarthan, M., Ramachandran, H., Chatterjee, M., 2012. Vanadium in cancer prevention. In: Vanadium: Biochemical and Molecular Biological Approaches, pp. 163–185.

De Domenico, I., Ward, D.M., Langelier, C., Vaughn, M.B., Nemeth, E., Sundquist, W.I., Ganz, T., Musci, G., Kaplan, J., 2007. The molecular mechanism of hepcidin-mediated ferroportin down-regulation. Mol. Biol. Cell 18, 2569–2578. https://doi.org/10.1091/mbc.e07-01-0060.

Denizot, F., Lang, R., 1986. Rapid colorimetric assay for cell growth and survival. Modifications to the tetrazolium dye procedure giving improved sensitivity and reliability. J. Immunol. Methods 89, 271–277. https://doi.org/10.1016/0022-1759(86)90368-6.

Domingo, J.L., Gomez, M., Llobet, J.M., Corbella, J., Keen, C.L., 1991. Oral vanadium administration to streptozotocin-diabetic rats has marked negative side-effects which are independent of the form of vanadium used. Toxicology 66, 279–287. https://doi.org/10.1016/0300-483X(91)90199-B.

Domingo, J.L., Gomez, M., Sanchez, D.J., Llobet, J.M., Keen, C.L., 1995. Toxicology of vanadium compounds in diabetic rats: the action of chelating agents on vanadium accumulation. Mol. Cell. Biochem. 153, 233–240. https://doi.org/10.1007/BF01075942.

Domingo, J.L., Gómez, M., 2016. Vanadium compounds for the treatment of human diabetes mellitus: a scientific curiosity? A review of thirty years of research. Food Chem. Toxicol. https://doi.org/10.1016/j.fct.2016.07.005.

Ekstrand, M.I., Falkenberg, M., Rantanen, A., Park, C.B., Gaspari, M., Hultenby, K., Rustin, P., Gustafsson, C.M., Larsson, N.G., 2004. Mitochondrial transcription factor A regulates mtDNA copy number in mammals. Hum. Mol. Genet. 13, 935–944. https://doi.org/10.1093/hmg/ddh109.

Fraqueza, G., Fuentes, J., Krivosudský, L., Dutta, S., Mal, S.S., Roller, A., Giester, G., Rompel, A., Aureliano, M., 2019. Inhibition of Na +/K + - and Ca 2+ -ATPase activities by phosphotetradecavanadate. J. Inorg. Biochem. https://doi.org/10.1016/j.jinorgbio.2019.110700.

Ghio, A.J., Piantadosi, C.A., Wang, X., Dailey, L.A., Stonehuerner, J.D., Madden, M.C., Yang, F., Dolan, K.G., Garrick, M.D., Garrick, L.M., 2005. Divalent metal transporter-1 decreases metal-related injury in the lung. Am. J. Physiol. Lung Cell Mol. Physiol. 289, L460–L467. https://doi.org/10.1152/ajplung.00154.2005.

Ghio, A.J., Stonehuerner, J., Soukup, J.M., Dailey, L.A., Kesic, M.J., Cohen, M.D., 2015. Iron diminishes the in vitro biological effect of vanadium. J. Inorg. Biochem. 147, 126–133. https://doi.org/10.1016/j.jinorgbio.2015.03.008.

Goldwaser, I., Gefel, D., Gershonov, E., Fridkin, M., Shechter, Y., 2000. Insulin-like effects of vanadium: basic and clinical implications. J. Inorg. Biochem. 80, 21–25. https://doi.org/10.1016/S0162-0134(00)00035-0.

Gumerova, N., Krivosudský, L., Fraqueza, G., Breibeck, J., Al-Sayed, E., Tanuhadi, E., Bijelic, A., Fuentes, J., Aureliano, M., Rompel, A., 2018. The P-type ATPase inhibiting potential of polyoxotungstates. Metallomics. https://doi.org/10.1039/c7mt00279c.

Gunshin, H., Mackenzie, B., Berger, U.V., Gunshin, Y., Romero, M.F., Boron, W.F., Nussberger, S., Gollan, J.L., Hediger, M.A., 1997. Cloning and characterization of a mammalian proton-coupled metal-ion transporter. Nature 388, 482–488. https://doi.org/10.1038/41343.

He, L., Chinnery, P.F., Durham, S.E., Blakely, E.L., Wardell, T.M., Borthwick, G.M., Taylor, R.W., Turnbull, D.M., 2002. Detection and quantification of mitochondrial DNA deletions in individual cells by real-time PCR. Nucleic Acids Res. 30, e68.

Horning, K.J., Caito, S.W., Tipps, K.G., Bowman, A.B., Aschner, M., 2015. Manganese is essential for neuronal health. Annu. Rev. Nutr. 35, 71–108. https://doi.org/10.1146/annurev-nutr-071714-034419.

Hosseini, M.J., Shaki, F., Ghazi-Khansari, M., Pourahmad, J., 2013. Toxicity of vanadium on isolated rat liver mitochondria: a new mechanistic approach. Metallomics 5, 152–166. https://doi.org/10.1039/c2mt20198d.

Iglesias-González, T., Sánchez-González, C., Montes-Bayón, M., Llopis-González, J., Sanz-Medel, A., 2012. Absorption, transport and insulin-mimetic properties of bis(maltolato)oxovanadium (IV) in streptozotocin-induced hyperglycemic rats by integrated mass spectrometric techniques. Anal. Bioanal. Chem. 402, 277–285. https://doi.org/10.1007/s00216-011-5286-7.

Kim, I., Rodriguez-Enriquez, S., Lemasters, J.J., 2007. Selective degradation of mitochondria by mitophagy. Arch. Biochem. Biophys. https://doi.org/10.1016/j.abb.2007.03.034.

Krośniak, M., Francik, R., Kowalska, J., Gryboś, R., Blusz, M., Kwiatek, W.M., 2013. Effects of vanadium complexes supplementation on V, Fe, Cu, Zn, Mn, Ca and K concentration in stz diabetic rat's spleen. Acta Pol. Pharm. Drug Res.

Lee, H.C., Wei, Y.H., 2005. Mitochondrial biogenesis and mitochondrial DNA maintenance of mammalian cells under oxidative stress. Int. J. Biochem. Cell Biol. 37, 822–834. https://doi.org/10.1016/j.biocel.2004.09.010.

Leopardi, P., Villani, P., Cordelli, E., Siniscalchi, E., Veschetti, E., Crebelli, R., 2005. Assessment of the in vivo genotoxicity of vanadate: analysis of micronuclei and DNA damage induced in mice by oral exposure. Toxicol. Lett. 158, 39–49. https://doi.org/10.1016/j.toxlet.2005.02.009.

Li, X., Xie, J., Lu, L., Zhang, L., Zhang, L., Zou, Y., Wang, Q., Luo, X., Li, S., 2013. Kinetics of manganese transport and gene expressions of manganese transport carriers in Caco-2 cell monolayers. Biometals 26, 941–953. https://doi.org/10.1007/s10534-013-9670-y.

Mackenzie, B., Takanaga, H., Hubert, N., Rolfs, A., Hediger, M.A., 2007. Functional properties of multiple isoforms of human divalent metal-ion transporter 1 (DMT1). Biochem. J. 403, 59–69. https://doi.org/10.1042/bj20061290.

McLauchlan, C.C., Hooker, J.D., Jones, M.A., Dymon, Z., Backhus, E.A., Greiner, B.A., Dorner, N.A., Youkhana, M.A., Manus, L.M., 2010. Inhibition of acid, alkaline, and tyrosine (PTP1B) phosphatases by novel vanadium complexes. J. Inorg. Biochem. 104, 274–281. https://doi.org/10.1016/j.jinorgbio.2009.12.001.

Nechay, B.R., Saunders, J.P., 1978. Inhibition by vanadium of sodium and potassium dependent adenosinetriphosphatase derived from animal and human tissues. J. Environ. Pathol. Toxicol. 2, 247–262.

Nemeth, E., Tuttle, M.S., Powelson, J., Vaughn, M.D., Donovan, A., Ward, D.M.V., Ganz, T., Kaplan, J., 2004. Hepcidin regulates cellular iron efflux by binding to ferroportin and inducing its internalization. Science (80) 306, 2090–2093. https://doi.org/10.1126/science.1104742.

Ochoa, J.J., Pamplona, R., Ramirez-Tortosa, M.C., Granados-Principal, S., Perez-Lopez, P., Naudí, A., Portero-Otin, M., López-Frías, M., Battino, M., Quiles, J.L., 2011. Age-related changes in brain mitochondrial DNA deletion and oxidative stress are differentially modulated by dietary fat type and coenzyme Q 10. Free Radic. Biol. Med. 50, 1053–1064. https://doi.org/10.1016/j.freeradbiomed.2011.02.004.

Oster, M.H., Llobet, J.M., Domingo, J.L., Bruce German, J., Keen, C.L., 1993. Vanadium treatment of diabetic Sprague-Dawley rats results in tissue vanadium accumulation and pro-oxidant effects. Toxicology 83, 115–130. https://doi.org/10.1016/0300-483X(93)90096-B.

Picard, M., Vincent, A.E., Turnbull, D.M., 2016. Expanding our understanding of mtDNA deletions. Cell Metabol. https://doi.org/10.1016/j.cmet.2016.06.024.

Pohjoismäki, J.L.O., Wanrooij, S., Hyvärinen, A.K., Goffart, S., Holt, I.J., Spelbrink, J.N., Jacobs, H.T., 2006. Alterations to the expression level of mitochondrial transcription factor A, TFAM, modify the mode of mitochondrial DNA replication in cultured human cells. Nucleic Acids Res. 34, 5815–5828. https://doi.org/10.1093/nar/gkl703.

Quiles, J.L., Ochoa, J.J., Ramirez-Tortosa, M.C., Huertas, J.R., Mataix, J., 2006. Age-related mitochondrial DNA deletion in rat liver depends on dietary fat unsaturation. Journals Gerontol. - Ser. A Biol. Sci. Med. Sci. 61, 107–114. https://doi.org/10.1093/gerona/61.2.107.

Quiles, J.L., Pamplona, R., Ramirez-Tortosa, M.C., Naudí, A., Portero-Otin, M., Araujo-Nepomuceno, E., López-Frías, M., Battino, M., Ochoa, J.J., 2010. Coenzyme Q addition to an n-6 PUFA-rich diet resembles benefits on age-related mitochondrial DNA deletion and oxidative stress of a MUFA-rich diet in rat heart. Mech. Ageing Dev. 131, 38–47. https://doi.org/10.1016/j.mad.2009.11.004.

Roy, S., Banerjee, S., Chakraborty, T., 2018. Vanadium quercetin complex attenuates mammary cancer by regulating the P53, Akt/mTOR pathway and downregulates cellular proliferation correlated with increased apoptotic events. Biometals 31, 647–671. https://doi.org/10.1007/s10534-018-0117-3.

Sanchez-Gonzalez, C., Bermudez-Peña, C., Trenzado, C.E., Goenaga-Infante, H., Montes-Bayon, M., Sanz-Medel, A., Llopis, J., 2012. Changes in the antioxidant defence and in selenium concentration in tissues of vanadium exposed rats. Metallomics. https://doi.org/10.1039/c2mt20066j.

Sánchez-González, C., Rivas-García, L., López-Chaves, C., Rodríguez-Nogales, A., Algieri, F., Gálvez, J., Gómez-Aracena, J., Vera-Ramírez, L., Montes-Bayon, M., Sanz-Medel, A., Llopis, J., 2014. Exposure to bis(maltolato)oxovanadium(IV) increases levels of hepcidin mRNA and impairs the homeostasis of iron but not that of manganese. Food Chem. Toxicol. https://doi.org/10.1016/j.fct.2014.08.011.

Ścibior, A., Zaporowska, H., Ostrowski, J., 2006. Selected haematological and biochemical parameters of blood in rats after subchronic administration of vanadium and/or magnesium in drinking water. Arch. Environ. Contam. Toxicol. 51, 287–295. https://doi.org/10.1007/s00244-005-0126-4.

Ścibior, A., Adamczyk, A., Gołębiowska, D., Niedźwiecka, I., 2012. Effect of 12-week vanadate and magnesium co-administration on chosen haematological parameters as well as on some indices of iron and copper metabolism and biomarkers of oxidative stress in rats. Environ. Toxicol. Pharmacol. 34. https://doi.org/10.1016/j.etap.2012.04.006.

Scibior, A., Adamczyk, A., Gołębiowska, D., Niedźwiecka, I., Fornal, E., 2014. The influence of combined magnesium and vanadate administration on the level of some elements in selected rat organs: V-Mg interactions and the role of iron-essential protein (DMT-1) in the mechanism underlying altered tissues iron level. Met. Integr. Biometal Sci. 6, 907–920. https://doi.org/10.1039/c3mt00363a.

Ścibior, A., Kurus, J., 2019. Vanadium and oxidative stress markers – in vivo model: a review. Curr. Med. Chem. https://doi.org/10.2174/0929867326666190108112255.

Shadel, G.S., 1997. Mitochondrial DNA maintenance in vertebrates. Annu. Rev. Biochem. 66, 409–435.

Sharma, P., Sampath, H., 2019. Mitochondrial DNA integrity: role in health and disease. Cells 8. https://doi.org/10.3390/cells8020100.

Soares, S.S., Martins, H., Duarte, R.O., Moura, J.J.G., Coucelo, J., Gutiérrez-Merino, C., Aureliano, M., 2007. Vanadium distribution, lipid peroxidation and oxidative stress markers upon decavanadate in vivo administration. J. Inorg. Biochem. 101, 80–88. https://doi.org/10.1016/j.jinorgbio.2006.08.002.

Thompson, K.H., Orvig, C., 2006. Vanadium in diabetes: 100 years from phase 0 to phase I. J. Inorg. Biochem. 100, 1925–1935. https://doi.org/10.1016/j.jinorgbio.2006.08.016.

Treviño, S., Díaz, A., Sánchez-Lara, E., Sanchez-Gaytan, B.L., Perez-Aguilar, J.M., González-Vergara, E., 2019. Vanadium in biological action: chemical, pharmacological aspects, and metabolic implications in diabetes mellitus. Biol. Trace Elem. Res. https://doi.org/10.1007/s12011-018-1540-6.

Vijaya Bharathi, B., Jaya Prakash, G., Krishna, K.M., Ravi Krishna, C.H., Sivanarayana, T., Madan, K., Rama Raju, G.A., Annapurna, A., 2015. Protective effect of alpha glucosyl hesperidin (G-hesperidin) on chronic vanadium induced testicular toxicity and sperm nuclear DNA damage in male Sprague Dawley rats. Andrologia 47, 568–578. https://doi.org/10.1111/and.12304.

Yamada, S., Nomoto, S., Fujii, T., Kaneko, T., Takeda, S., Inoue, S., Kanazumi, N., Nakao, A., 2006. Correlation between copy number of mitochondrial DNA and clinico-pathologic parameters of hepatocellular carcinoma. Eur. J. Surg. Oncol. 32, 303–307. https://doi.org/10.1016/j.ejso.2006.01.002.

Yu, M., 2011. Generation, function and diagnostic value of mitochondrial DNA copy number alterations in human cancers. Life Sci. https://doi.org/10.1016/j.lfs.2011.05.010.

Zhao, Y., Ye, L., Liu, H., Xia, Q., Zhang, Y., Yang, X., Wang, K., 2010. Vanadium compounds induced mitochondria permeability transition pore (PTP) opening related to oxidative stress. J. Inorg. Biochem. 104, 371–378. https://doi.org/10.1016/j.jinorgbio.2009.11.007.